
DYNAMIC UNIVERSAL APPROXIMATION THEORY: THE BASIC THEORY FOR RESIDUAL-BASED DEEP LEARNING COMPUTER VISION MODELS

Wei Wang

Department of Comp
The Hong Kong Polytechnic University
weiuat.wang@connect.polyu.hk

Qing Li

Department of Comp
The Hong Kong Polytechnic University
qing-prof.li@polyu.edu.hk

ABSTRACT

Computer Vision (CV) is one of the most critical branches in artificial intelligence. In recent years, various deep learning models based on convolutional architectures and Transformers have been developed to address diverse challenges in CV. These algorithms have found practical applications in fields such as robotics and facial recognition. Despite the increasing capabilities of modern CV models, several fundamental questions remain unresolved. For instance, what underpins the generalization ability of Convolutional Neural Networks (CNNs)? The root of these issues lies in the lack of a robust theoretical foundation for deep learning models in CV. To address these key challenges, we propose the Dynamic Universal Approximation Theorem (DUAT), an advance of the Universal Approximation Theorem (UAT). We demonstrate that most residual-based deep learning models in CV fall under the category of DUAT functions. By doing so, we aim to clarify some theoretical issues in CV.

1 INTRODUCTION

As a core branch of artificial intelligence, CV has a wide range of applications, encompassing tasks such as image segmentation Minaee et al. (2021); Wang et al. (2022a), classification Rawat & Wang (2017); Wang et al. (2017), video synthesis Wang et al. (2018; 2019a), and restoration Wang et al. (2019b); Nah et al. (2019). This broad applicability highlights its enormous technical potential and practical significance, making the intelligent processing of CV tasks a highly important area of research. The most effective solutions in this field today are based on deep learning algorithms.

One of the earliest and most influential works in using deep learning for CV was LeNet Lecun et al. (1998), which pioneered the use of CNNs for handwritten digit recognition, ushering in a new era of image processing. Following this, AlexNet’s Krizhevsky et al. (2017) remarkable performance on the ImageNet Russakovsky et al. (2014) dataset not only achieved a significant leap in image classification accuracy but also cemented CNNs as the dominant method in visual processing. The subsequent introduction of ResNet He et al. (2016) further improved image recognition accuracy and established residual-based structure as a foundational architecture for future network designs, influencing nearly all subsequent deep learning models Ren et al. (2015); Xie et al. (2016); Szegedy et al. (2014); Gao et al. (2019); Liu et al. (2021).

In recent years, the success of Transformers Vaswani et al. (2017) in the field of natural language processing (NLP) has gradually permeated CV. Researchers have begun designing models for CV based on Transformers, such as the Vision Transformer (ViT) Dosovitskiy et al. (2020), Swin Transformer Liu et al. (2021) and StructViT Kim et al. (2024), which have demonstrated capabilities comparable to CNNs in image tasks (For convenience, we collectively refer to all Transformer-based models in the CV domain as ViTs.). Currently, research in deep learning for image processing predominantly revolves around CNNs Huang et al. (2023); Wang et al. (2022b), Transformers Shi (2023); Wang et al. (2023), or strategies that integrate both Lv et al. (2023); Hou et al. (2024), continuously driving technological advancements.

Despite the significant advances in deep learning-based computer vision, several fundamental questions remain unanswered. For instance, why do CNNs require such deep architectures? What underpins the generalization ability of CNNs? Why do residual networks outperform fully convolutional networks like VGG Simonyan & Zisserman (2014)? What are the core differences between residual-based CNNs and Transformer-based models? We believe that these questions arise from the lack of a foundational theory for CNNs.

While some researchers have attempted to explain CNNs through various approaches—such as using visualization techniques to analyze the relationship between feature maps and original images Wei et al. (2016) or exploring CNNs from the frequency domain perspective Yin et al. (2019); Xu et al. (2019)—these explanations often have limitations and are somewhat subjective. Similarly, studies on the interpretability of ViTs Park & Kim (2022); Bai et al. (2022) suggest that the multi-head attention (MHA) mechanism in Transformers tends to capture low-frequency information, in contrast to CNNs, which function as high-pass filters. These studies advocate for combining the strengths of both models or improving ViTs to better capture high-frequency details. However, these methods only provide intuitive explanations for specific problems and fail to offer a theoretical framework for addressing broader issues within CNNs and ViTs. Essentially, they describe or interpret phenomena occurring within CNNs or ViTs rather than providing a comprehensive theory for these architectures.

To address these challenges, we propose the DUAT, which applies to both residual-based CNNs and ViTs. DUAT is an advancement of the UAT, specifically developed to address the commonly used residual structures in deep learning models for computer vision. Although previous studies Lin et al. (2022); Yang et al. (2024); Zhou (2018; 2020) have attempted to use UAT to explain certain aspects of CNNs, they are often limited by specific conditions, lacking broad applicability or practical guidance. For example, these studies have not fundamentally clarified the differences between residual-based CNNs and VGG, nor have they extended to ViTs.

Our objective is to employ the Matrix-Vector Method introduced in DUAT2LLMs Wang & Li (2024a) to demonstrate that both residual-based CNNs and ViTs fall within the class of DUAT functions, theoretically resolving the aforementioned issues and providing practical insights for network design Wang & Li (2024b). Our contributions are as follows:

- We further developed the UAT to DUAT, which could help explain some problems in the CV area.
- We demonstrate that the residual-based multi-layer convolutional and Transformer networks commonly employed in the field of CV belong to the DUAT function.
- We explained why CNNs require deep networks, considering the characteristics of image data and the DUAT perspective.
- We proved why the widely used residual structure in CV is so powerful beyond the full convolutional networks, like VGG.
- We generally compared a residual-based CNN and a ViT from the DUAT perspective, illustrating the source of their powerful capabilities and explaining why both models appear to have similar performance.

The structure of this paper is as follows: In Section 2, we introduce the UAT and the Matrix-Vector Method, as well as DUAT. In Section 3, we use the Matrix-Vector Method to transform some commonly used operations in CV into matrix-vector forms, such as 2D convolution (3.1), 3D convolution (3.2), mean-pooling (3.3), and then we give the DUAT format of residual-based CNNs (3.4) and ViTs (3.5). In Section 4, we address some fundamental questions in CV: why CNN networks need to be deep (4.1), why residual-based CNNs are more powerful than VGG (4.2) and the differences between residual-based CNNs and ViTs (4.3).

2 FROM UAT TO DUAT

Our goal is to unify residual-based CNNs and ViTs within the DUAT framework, where DUAT can be seen as an advanced form of UAT. Before introducing DUAT, we first provide an overview of UAT and briefly describe the Matrix-Vector Method proposed in DUAT2LLMs Wang & Li (2024a).

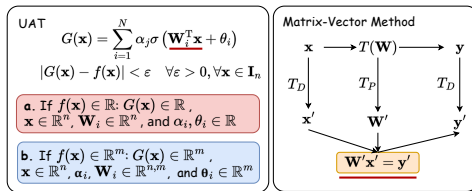


Figure 1: The basic format of UAT and The Matrix-Vector Method and their relationship.

Figure 1 offers a simplified overview from DUAT2LLMs. Here, $G(\mathbf{x})$ represents the general form of UAT, which approximates Borel-measurable functions over closed intervals Cybenko (1989); Hornik et al. (1989), with \mathbf{I}_n denoting the n -dimensional unit cube. UAT extends from one-dimensional to multi-dimensional approximations, illustrated in Figures 1.a and 1.b. The fundamental computational unit of UAT is expressed as $\alpha_j \sigma(\mathbf{W}_j^T \mathbf{x} + \theta_j)$. $\mathbf{W}_j^T \mathbf{x} + \theta_j$ can be interpreted as convolution and pooling operations in CNNs, or as MHA and linear operations in ViTs, the specific mathematical forms of these basic operations differ from $\mathbf{W}_j^T \mathbf{x} + \theta_j$. To bridge this gap, the matrix-vector approach is introduced.

The right of Figure 1 illustrates how these operations can be transformed into a matrix-vector multiplication form, $\mathbf{W}_j^T \mathbf{x} + \theta_j$, using the Matrix-Vector Method. In this context, T represents various transformations within CNNs and ViTs, while T_D and T_P denote specific matrix-vector transformations, varying with the choice of T . These transformations require converting input data \mathbf{x} , output data \mathbf{y} , and parameters \mathbf{W} into their vectorized forms \mathbf{x}' , \mathbf{y}' , and parameter matrix \mathbf{W}' . These transformations ensure the computational relation $\mathbf{W}'\mathbf{x}' = \mathbf{y}'$, as shown in Figure 1. We use a prime symbol $'$ to indicate the matrix-vector representations of these transformed variables, distinguishing them from their original forms. This establishes the link between basic network operations and $\mathbf{W}_j^T \mathbf{x} + \theta_j$ (notably, we omit the bias term for simplification, focusing on basic operations' transformations, like convolution).

With this connection established between network basic operations and UAT's basic computational units, what about multi-layer networks? By expressing multi-layer networks mathematically in matrix-vector form, we observe that fully convolutional networks align with UAT in mathematical format (we illustrate this using the VGG network's mathematical form in Section 4.2). As most current CV networks employ residual connections, writing these networks in corresponding mathematical terms reveals that their overall mathematical format aligns with UAT. However, unlike classic UAT, most parameters in these formulas vary with the input, making them functions of the input. We define this form of UAT, where some or all parameters depend on the input, as DUAT. (In Section 3.4 and 3.5, we present the DUAT mathematical form for a multi-layer residual-based CNN and ViT.) To demonstrate that a multi-layer network qualifies as DUAT, we use the matrix-vector method to represent the mathematical form of these networks, establish their consistency with UAT, and verify that certain UAT parameters vary dynamically with the input, confirming them as DUAT functions. Through the introduction of DUAT, we aim to address unresolved questions in computer vision.

3 THE DUAT FORMAT OF CNNs AND ViTs

In the previous sections, we explained that to unify CNNs and ViTs under the DUAT, it is necessary to demonstrate that their various transformations (convolution, mean pooling, MHA, and linear) can be represented in matrix-vector form. DUAT2LLMs has already shown how to represent MHA and linear in matrix-vector form. Therefore, in this section, we will specifically demonstrate how to convert convolution and mean pooling in CNNs into matrix-vector form using the Matrix-Vector Method. Additionally, we will interpret the unique aspects of Transformer within the context of CV. In the end, we give the DUAT format of residual-based CNNs and ViTs.

Considering that convolution in CV can be either 2D or 3D and that the input and output may consist of single or multiple channels. We use the notation \mathbf{I} to represent a single channel, \mathbf{I} to represent an input with \mathbf{I} channels, and \mathbf{O} to represent an output with \mathbf{O} channels. For example, $\mathbf{1-O}$ indicates an operation with one channel input and \mathbf{O} channels output. Below, we will show how to convert these

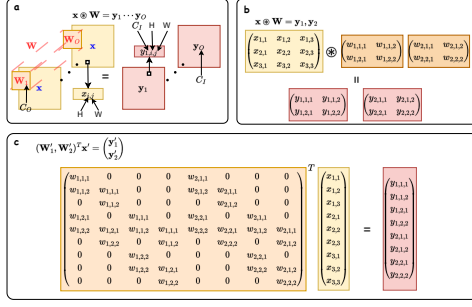


Figure 2: 1-O Conv2D process and the matrix-vector transformation example. In **a**, we present the operation of 1-O Conv2D. At the top of **a**, **b** and **c**, we provide the mathematical formula corresponding to the diagram. Additionally, we group the variables in the figure, such as $W = \text{Concat}(W_1, \dots, W_O)$. In **b**, we provide an example corresponding to **a**, and in **c**, we show the matrix-vector form of the example given in **b**. The following figures follow the same conventions.

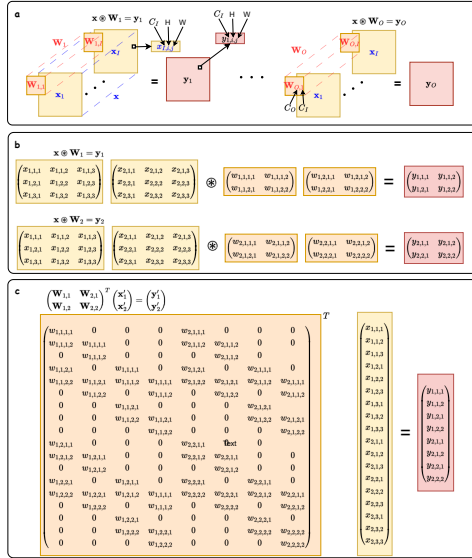


Figure 3: I-O Conv2D process and the matrix-vector transformation example.

transformations into the corresponding matrix-vector forms. Then we will give the DUAT format of residual-based CNNs and ViTs.

3.1 THE MATRIX-VECTOR METHOD FOR CONV2D

In this section, we will detail how to convert 2D convolution into its corresponding matrix-vector forms, focusing on two scenarios: 1-O and I-O. To clearly describe the 2D convolution process, we first outline the general procedure and some basic conventions. The general process of 2D convolution involves convolving a kernel with the input data and then summing along the input channel direction (referred to as the C_I direction) to obtain an element in the output. The convolution kernel slides along the height (H) and width (W) directions to produce the entire output feature map. To generate multiple feature maps, multiple sets of convolution kernels, C_O , are required, with each set having the same number of channels as the input channels. Depending on the context, C_I , C_O , H , and W can represent either the corresponding dimension directions or the number of dimensions in those directions. Figures 2 and 3 illustrate the conversion process for the cases of 1-O and I-O, transforming them into matrix-vector representations.

Specifically, Figure 2.a shows the process of 1-O Conv2D. Here, $W_1 \dots W_O$ represent the convolution kernels, which slide across the input data along the H and W directions. For a single-channel

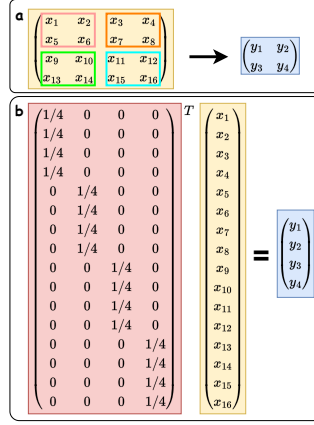


Figure 6: Mean pooling process and the matrix-vector transformation example. Pink, orange, green and blue boxes represent mean pooling size.

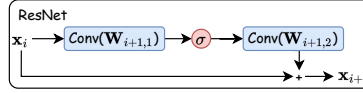


Figure 7: A general residual module in ResNet.

3.3 THE MATRIX-VECTOR METHOD FOR MEAN POOLING

Mean pooling is also an important technique in the field of CV, often used in conjunction with convolution. To demonstrate that CNNs can be expressed in the form of UAT, we need to prove that mean pooling can also be represented in matrix-vector form. In Figure 6, we provide an example. Figure 6.a shows the process of mean pooling, while Figure 6.b illustrates its corresponding matrix-vector form. Based on Figure 6, we can conclude that mean pooling can indeed be represented in matrix-vector form.

3.4 THE DUAT FORMAT OF RESIDUAL-BASED CNNs

Building on the previous derivation, we know that almost all types of basic operations in CNNs can be expressed in matrix-vector form. Here, we present the DUAT formulation for a general multi-layer residual-based CNN. Assuming a basic residual CNN module as shown in Figure 7, the DUAT form for a multi-layer residual-based CNN can be expressed as follows (for detailed deduction, refer to [Appendix A.3](#)):

$$\mathbf{x}'_{i+1} = (\mathbf{x}'_0 + \mathbf{b}'_{i+1,2}) + \sum_{j=1}^{i+1} \mathbf{W}'_{j,2} \sigma(\mathbf{W}'_{j,1} \mathbf{x}'_0 + \mathbf{b}'_{j,1}) \quad (3)$$

where $i = 0, 1, 2, \dots$. For $i = 0$, we have $\mathbf{b}'_{1,1} = \mathbf{b}'_{1,1}$; and for $i > 0$, $\mathbf{b}'_{j,1}$ is defined by $\mathbf{b}'_{j,1} = (\mathbf{W}'_{j,1} \mathbf{b}'_{j-1,2} + \mathbf{b}'_{j,1}) + \mathbf{W}'_{j,1} \sum_{k=1}^{j-1} \mathbf{W}'_{k,2} \sigma(\mathbf{W}'_{k,1} \mathbf{x}'_0 + \mathbf{b}'_{k,1})$. Thus, $\mathbf{b}'_{j,1}$ can be seen as a j -layer UAT and the input is \mathbf{x}'_0 . For convenience, we also consider the first term as part of the UAT. Additionally, for the term $\mathbf{b}'_{j+1,2}$ at layer i , it is given by $\mathbf{b}'_{j+1,2} = \mathbf{b}'_{1,2} \cdots \mathbf{b}'_{j,2} + \mathbf{b}'_{j+1,2}, j = 1, 2 \cdots i$. Eq. 3 aligns with the UAT form, as illustrated in Figure 1. In this context, $\mathbf{b}'_{j,1}$ functions as a dynamic parameter that is approximated through UAT. Consequently, Eq. 3 satisfies the DUAT criterion, adopting a UAT form where the parameters dynamically adapt to the input.

3.5 THE DUAT FORMAT OF ViTs

In DUAT2LLMs, it has been demonstrated that the feedforward network (FFN) and MHA components in the Transformer architecture can be represented in matrix-vector form. Given that ViTs are also based on the Transformer framework, we only need to focus on the differences between Transformers in CV and those in LLMs. A key feature of ViTs is that they divide the original

image into multiple patches: $\mathbf{x}_{1,1}, \dots, \mathbf{x}_{n,m}$. Each image patch is then reshaped into row vectors $\bar{\mathbf{x}}_{1,1}, \dots, \bar{\mathbf{x}}_{n,m}$, which are concatenated along the column direction to obtain $\bar{\mathbf{x}}$, as shown in Figure 8. MHA and FFN operations are then applied, so aside from the initial processing part, the subsequent transformation process completely follows the description in DUAT2LLMs.

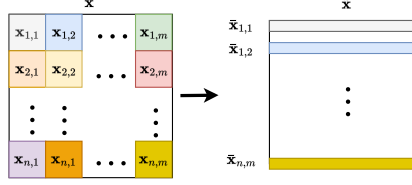


Figure 8: The MHA operation in CV.

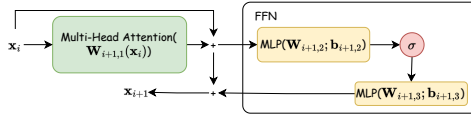


Figure 9: The process of Transformer.

Therefore, a multi-layer ViT structured in Figure 9 can be expressed as:

$$\mathbf{x}_{i+1} = (\mathbf{W}'_{i+1,1}\mathbf{x}_0 + \mathbf{b}'_{i+1,3}) + \sum_{j=1}^{i+1} \mathbf{W}'_{j,3}\sigma(\mathbf{W}'_{j,2}\mathbf{x}'_0 + \mathbf{b}'_{j,2}) \quad (4)$$

When $i = 0$, the parameters are defined as follows: $\mathbf{W}'_{1,1} = \mathbf{W}'_{1,1}$, $\mathbf{b}'_{1,3} = \mathbf{b}'_{1,3}$, $\mathbf{W}'_{1,3} = \mathbf{W}'_{1,3}$, $\mathbf{W}'_{1,2} = \mathbf{W}'_{1,2}\mathbf{W}'_{1,1}$, and $\mathbf{b}'_{1,2} = \mathbf{b}'_{1,2}$. We define the parameters for cases where $i \geq 1$. For each $j = 1, 2, \dots, i$, the updates are as follows: $\mathbf{W}'_{j+1,1} = \mathbf{W}'_{j+1,1}\mathbf{W}'_{j,1}$, $\mathbf{b}'_{j+1,3} = \mathbf{W}'_{j+1,1}\mathbf{b}'_{j,3} + \mathbf{b}'_{j+1,3}$, $\mathbf{W}'_{j+1,2} = \mathbf{W}'_{j+1,2}\mathbf{W}'_{j,1}$, and $\mathbf{W}'_{j,3} = \mathbf{W}'_{j+1,1}\mathbf{W}'_{j,3}$. Additionally, for $j = 2, \dots, i+1$, the bias terms $\mathbf{b}'_{j,2}$ are updated according to:

$$\begin{aligned} \mathbf{b}'_{j,2} = & (\mathbf{W}'_{j,2}\mathbf{b}'_{j-1,3} + \mathbf{b}'_{j,2}) \\ & + \mathbf{W}'_{j,2} \sum_{k=1}^{j-1} \mathbf{W}'_{k,3}\sigma(\mathbf{W}'_{k,2}\mathbf{x}'_0 + \mathbf{b}'_{k,2}). \end{aligned} \quad (5)$$

It means that the whole computing process is serial, if we want to compute $\mathbf{W}'_{3,1}$, we must calculate $\mathbf{W}'_{2,1}$, because $\mathbf{W}'_{3,1} = \mathbf{W}'_{3,1}\mathbf{W}'_{2,1}$. Thus, we have established that a multilayer ViT is also a DUAT function. The mathematical representation of the ViT aligns with the DUAT framework, with $\mathbf{b}'_{j,2}$ closely approximated by DUAT. The most notable difference between ViTs and residual-based CNNs is the dynamic input-dependent nature of the parameters in the MHA mechanism. Consequently, in the DUAT formulation associated with ViT, the parameters $\mathbf{W}'_{j,1}$ and $\mathbf{W}'_{j,2}$ for $i+1 \geq j \geq 1$, and $\mathbf{W}'_{j,3}$ for $i+1 > j > 1$ in layer i , all adapt dynamically based on the input. For further details, please refer to [Appendix A.4](#).

4 DISCUSSION

In this section, we will answer the questions in the field of CV proposed in the Introduction.

4.1 WHY MUST CNNs BE DEEP?

There are two main reasons why CNNs typically have deep layers. The first reason stems from the learning paradigm of CNNs. The design of CNNs is based on two well-known principles: local receptive fields (i.e., local features in images often contain important information) and spatial invariance (these important local features can appear anywhere in the image). These principles necessitate

learning from each small region of the image, with all small regions sharing the same parameters. If parameters differed, it would imply that a certain object must appear in a specific part of the image, which is clearly unreasonable.

The above reasons dictate that image learning occurs in small patches, which explains why convolutional kernels are typically small. However, if the network has only a few layers, such as a single layer, it means that each small patch is learned independently. We know that objects in an image are generally composed of multiple such patches. Observing only a part of the image cannot provide a clear identification of the object. Therefore, a larger receptive field is needed, which can be achieved by increasing the number of layers to gather global information.

The second reason is derived from the DUAT. As shown in Figure 1, increasing the number of layers in the network means a larger N , which brings the DUAT closer to approximating the target function. An image can be understood as a special function in a high-dimensional space, exhibiting strong correlations in 2D or 3D space. These two reasons are also applicable to ViTs. Figure 8 shows the preprocessing of ViTs, where $\tilde{\mathbf{x}}$ is the input to the ViTs. It is evident that each row shares the same parameters, and the learning of each row adheres to the principles of local receptive fields and spatial invariance.

4.2 WHY RESIDUAL-BASED CNNs EXCEL IN CV: SUPERIOR GENERALIZATION ABILITY

In the previous discussion, we explained why deep networks are essential for learning in CNNs. However, why did VGG, despite being a deep network, not dominate the subsequent development of CV, whereas residual-based CNNs did? ResNet significantly shaped the design of later network architectures, with the residual structure appearing in many subsequent networks. What exactly endows the residual structure with such powerful capabilities? We think the answer is the generalization capability given by residual structure. To analyze the source of this power, we use the Matrix-Vector Method to express VGG and the residual-based CNNs into equations, and then compare them.

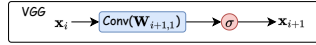


Figure 10: VGG: The characters in ‘()’ represent the corresponding operation’s parameters.

Figure 10 illustrates a basic structure of VGG. Based on this figure, a i -layer VGG can be written as:

$$\mathbf{x}'_i = \sigma\{\mathbf{W}'_i \cdots \sigma\{\mathbf{W}'_3 [\sigma(\mathbf{W}'_2 \sigma(\mathbf{W}'_1 \mathbf{x}'_1 + \mathbf{b}'_1) + \mathbf{b}'_2)] + \mathbf{b}'_3\} + \mathbf{b}'_i\} \quad (6)$$

which perfectly aligns with the mathematical formulation of the multilayer UAT proposed by Hornik et al. (1989). Therefore, based on Eqs. 6 and 3, we can conclude that the fundamental reason ResNet is more powerful than VGG lies in the fact that the residual network is a DUAT function, while VGG is a UAT function. DUAT has a stronger dynamic approximation capability. As shown in Eq. 6, once the VGG network finishes the training, its corresponding UAT parameters become fixed. This means that the VGG network can only approximate a single, fixed function. Although UAT has strong approximation capabilities, image data is highly variable, and the corresponding functions often change.

In contrast, the residual network, corresponding to the DUAT in Eq. 3, can dynamically adjust its bias parameters based on the input, allowing it to approximate the corresponding function dynamically. This adaptability is the fundamental source of the superiority of residual networks.

4.3 THE DIFFERENCE BETWEEN RESIDUAL-BASED CNNs AND ViTs

In this section, we will compare the DUAT format of Transformer-based ViTs and residual-based CNNs. Figure 9 shows the general form of a Transformer. A multi-layer Transformer is shown in Eq 4. Comparing Eq. 4 and 3, the main difference between Transformer networks and residual-based multi-layer convolutional networks lies in how the input affects their corresponding DUAT

parameters. In Transformer networks, input information influences both weight and bias in the corresponding DUAT. In contrast, in networks constructed with residual-based CNNs, input information only influences bias in the corresponding DUAT. Essentially, both types of networks have the ability to dynamically approximate functions based on input. This aligns with their nearly identical performance in the field of CV, supporting the theoretical foundation that both are DUAT functions and capable of dynamically approximating the corresponding functions based on input.

5 CONCLUSION

This paper delves into the theoretical foundations of deep learning in the field of CV. Specifically, the current CV landscape is primarily dominated by CNNs and Transformer models. We utilize the Matrix-Vector Method to unify these models under the framework of the DUAT. Based on this framework, we provide explanations for several common issues and techniques in CV. The requirement for deep networks in CNNs is jointly determined by the intrinsic characteristics of image data and the demands of DUAT. The robust generalization ability of residual networks stems from their ingenious design, which enables UAT to dynamically adapt to corresponding functions based on input data. Similarly, Transformer-based models possess this ability, with the key difference lying in which parameters of UAT they influence. Residual networks primarily affect the bias term, while Transformers influence both the weights and the bias.

6 SOME GUESSES ON HUMAN VISION BASED ON DUAT

Based on the above discussion, we can consider that residual-based deep learning CV models are DUAT functions, which we refer to as DUAT vision. So, what is the relationship between human vision and DUAT vision? We believe that the human brain functions as a large network composed of one or multiple DUATs. Because first neural network is perceptron Rosenblatt (1963) which was designed based on the brain neuron. The Transformer and residual-based CNNs are DUAT functions, and the perceptron can be seen as a special form of UAT. Therefore, the concepts of memory and understanding, as defined by humans, can be categorized as reasoning based on the DUAT in our brains. Just as deep vision networks do not have a database storing images, they directly approximate the corresponding results from the inputs (which can be simplified as $y = DUAT(x)$). Specifically, humans and animals are born with certain weights in their brains, which are innate reflexes, such as infants instinctively knowing how to suckle. However, other weights in the brain need to be learned, and our process of observing the world from a young age is essentially a process of training these weights. Given that the eyes' vision operates at 30 frames per second Lu et al. (2017), the brain would be trained on hundreds of millions of high-resolution images over a year.

So, what is human memory? We believe it is the ability to generate corresponding results based on inputs and the weights learned by the brain. The so-called memory always has an anchor point that triggers it, i.e., something that evokes the memory. For example, an object might remind us of childhood memories because the visual input is similar or identical to what we saw in our childhood. We then derive a memory image, which is input back into the brain, and iterated repeatedly until the entire memory fragment is formed. Memory bias occurs when the brain's weight parameters are updated, leading to different results from the same input. Since the brain's weights are trained based on the natural world, it only infers results that are reasonable within the realm of cognition. This is why it is challenging for us to imagine things that do not exist, as the weights related to images in our brains are trained based on the natural world.

REFERENCES

- Jiawang Bai, Li Yuan, Shu-Tao Xia, Shuicheng Yan, Zhifeng Li, and Wei Liu. Improving vision transformers by revisiting high-frequency components. In *European Conference on Computer Vision*, pp. 1–18. Springer, 2022.
- George V. Cybenko. Approximation by superpositions of a sigmoidal function. *Mathematics of Control, Signals and Systems*, 2:303–314, 1989. URL <https://api.semanticscholar.org/CorpusID:3958369>.

-
- Alexey Dosovitskiy, Lucas Beyer, Alexander Kolesnikov, Dirk Weissenborn, Xiaohua Zhai, Thomas Unterthiner, Mostafa Dehghani, Matthias Minderer, Georg Heigold, Sylvain Gelly, et al. An image is worth 16x16 words: Transformers for image recognition at scale. *arXiv preprint arXiv:2010.11929*, 2020.
- Shanghua Gao, Ming-Ming Cheng, Kai Zhao, Xinyu Zhang, Ming-Hsuan Yang, and Philip H. S. Torr. Res2net: A new multi-scale backbone architecture. *IEEE Transactions on Pattern Analysis and Machine Intelligence*, 43:652–662, 2019. URL <https://api.semanticscholar.org/CorpusID:91184391>.
- Kaiming He, Xiangyu Zhang, Shaoqing Ren, and Jian Sun. Deep residual learning for image recognition. In *Proceedings of the IEEE conference on computer vision and pattern recognition*, pp. 770–778, 2016.
- Kurt Hornik, Maxwell B. Stinchcombe, and Halbert L. White. Multilayer feedforward networks are universal approximators. *Neural Networks*, 2:359–366, 1989. URL <https://api.semanticscholar.org/CorpusID:2757547>.
- Xiuquan Hou, Meiqin Liu, Senlin Zhang, Ping Wei, and Badong Chen. Saliency detr: Enhancing detection transformer with hierarchical saliency filtering refinement. *ArXiv*, abs/2403.16131, 2024. URL <https://api.semanticscholar.org/CorpusID:268680782>.
- Tianjin Huang, Lu Yin, Zhenyu (Allen) Zhang, Lijuan Shen, Meng Fang, Mykola Pechenizkiy, Zhangyang Wang, and Shiwei Liu. Are large kernels better teachers than transformers for convnets? In *International Conference on Machine Learning*, 2023. URL <https://api.semanticscholar.org/CorpusID:258987774>.
- Manjin Kim, Paul Hongsuck Seo, Cordelia Schmid, and Minsu Cho. Learning correlation structures for vision transformers. *ArXiv*, abs/2404.03924, 2024. URL <https://api.semanticscholar.org/CorpusID:268987591>.
- Alex Krizhevsky, Ilya Sutskever, and Geoffrey E. Hinton. Imagenet classification with deep convolutional neural networks. *Commun. ACM*, 60(6):84–90, may 2017. ISSN 0001-0782. doi: 10.1145/3065386. URL <https://doi.org/10.1145/3065386>.
- Y. Lecun, L. Bottou, Y. Bengio, and P. Haffner. Gradient-based learning applied to document recognition. *Proceedings of the IEEE*, 86(11):2278–2324, 1998. doi: 10.1109/5.726791.
- Ting-Wei Lin, Zuowei Shen, and Qianxiao Li. On the universal approximation property of deep fully convolutional neural networks. *ArXiv*, abs/2211.14047, 2022. URL <https://api.semanticscholar.org/CorpusID:254017581>.
- Ze Liu, Yutong Lin, Yue Cao, Han Hu, Yixuan Wei, Zheng Zhang, Stephen Lin, and Baining Guo. Swin transformer: Hierarchical vision transformer using shifted windows. *2021 IEEE/CVF International Conference on Computer Vision (ICCV)*, pp. 9992–10002, 2021. URL <https://api.semanticscholar.org/CorpusID:232352874>.
- Jing Lu, Boyu Gu, Xiaolin Wang, and Yuhua Zhang. High-speed adaptive optics line scan confocal retinal imaging for human eye. *PloS one*, 12(3):e0169358, 2017.
- Wenyu Lv, Shangliang Xu, Yian Zhao, Guanzhong Wang, Jinman Wei, Cheng Cui, Yuning Du, Qingqing Dang, and Yi Liu. Detsr beat yolos on real-time object detection. *ArXiv*, abs/2304.08069, 2023. URL <https://api.semanticscholar.org/CorpusID:258179840>.
- Shervin Minaee, Yuri Boykov, Fatih Porikli, Antonio Plaza, Nasser Kehtarnavaz, and Demetri Terzopoulos. Image segmentation using deep learning: A survey. *IEEE transactions on pattern analysis and machine intelligence*, 44(7):3523–3542, 2021.
- Seungjun Nah, Sungyong Baik, Seokil Hong, Gyeongsik Moon, Sanghyun Son, Radu Timofte, and Kyoung Mu Lee. Ntire 2019 challenge on video deblurring and super-resolution: Dataset and study. In *Proceedings of the IEEE/CVF conference on computer vision and pattern recognition workshops*, pp. 0–0, 2019.

-
- Namuk Park and Songkuk Kim. How do vision transformers work? *arXiv preprint arXiv:2202.06709*, 2022.
- Waseem Rawat and Zenghui Wang. Deep convolutional neural networks for image classification: A comprehensive review. *Neural computation*, 29(9):2352–2449, 2017.
- Shaoqing Ren, Kaiming He, Ross B. Girshick, and Jian Sun. Faster r-cnn: Towards real-time object detection with region proposal networks. *IEEE Transactions on Pattern Analysis and Machine Intelligence*, 39:1137–1149, 2015. URL <https://api.semanticscholar.org/CorpusID:10328909>.
- Frank Rosenblatt. Principles of neurodynamics. perceptrons and the theory of brain mechanisms. *American Journal of Psychology*, 76:705, 1963. URL <https://api.semanticscholar.org/CorpusID:62710001>.
- Olga Russakovsky, Jia Deng, Hao Su, Jonathan Krause, Sanjeev Satheesh, Sean Ma, Zhiheng Huang, Andrej Karpathy, Aditya Khosla, Michael S. Bernstein, Alexander C. Berg, and Li Fei-Fei. Imagenet large scale visual recognition challenge. *International Journal of Computer Vision*, 115:211 – 252, 2014. URL <https://api.semanticscholar.org/CorpusID:2930547>.
- Dai Shi. Transnext: Robust foveal visual perception for vision transformers. *ArXiv*, abs/2311.17132, 2023. URL <https://api.semanticscholar.org/CorpusID:265498825>.
- Karen Simonyan and Andrew Zisserman. Very deep convolutional networks for large-scale image recognition. *CoRR*, abs/1409.1556, 2014. URL <https://api.semanticscholar.org/CorpusID:14124313>.
- Christian Szegedy, Wei Liu, Yangqing Jia, Pierre Sermanet, Scott E. Reed, Dragomir Anguelov, D. Erhan, Vincent Vanhoucke, and Andrew Rabinovich. Going deeper with convolutions. *2015 IEEE Conference on Computer Vision and Pattern Recognition (CVPR)*, pp. 1–9, 2014. URL <https://api.semanticscholar.org/CorpusID:206592484>.
- Ashish Vaswani, Noam M. Shazeer, Niki Parmar, Jakob Uszkoreit, Llion Jones, Aidan N. Gomez, Lukasz Kaiser, and Illia Polosukhin. Attention is all you need. In *Neural Information Processing Systems*, 2017. URL <https://api.semanticscholar.org/CorpusID:13756489>.
- Ao Wang, Hui Chen, Zijia Lin, Hengjun Pu, and Guiguang Ding. Repvit: Revisiting mobile cnn from vit perspective. *ArXiv*, abs/2307.09283, 2023. URL <https://api.semanticscholar.org/CorpusID:259951457>.
- Fei Wang, Mengqing Jiang, Chen Qian, Shuo Yang, Cheng Li, Honggang Zhang, Xiaogang Wang, and Xiaoou Tang. Residual attention network for image classification. In *Proceedings of the IEEE conference on computer vision and pattern recognition*, pp. 3156–3164, 2017.
- Risheng Wang, Tao Lei, Ruixia Cui, Bingtao Zhang, Hongying Meng, and Asoke K Nandi. Medical image segmentation using deep learning: A survey. *IET Image Processing*, 16(5):1243–1267, 2022a.
- Ting-Chun Wang, Ming-Yu Liu, Jun-Yan Zhu, Guilin Liu, Andrew Tao, Jan Kautz, and Bryan Catanzaro. Video-to-video synthesis. *arXiv preprint arXiv:1808.06601*, 2018.
- Ting-Chun Wang, Ming-Yu Liu, Andrew Tao, Guilin Liu, Jan Kautz, and Bryan Catanzaro. Few-shot video-to-video synthesis. *arXiv preprint arXiv:1910.12713*, 2019a.
- Wei Wang and Qing Li. Universal approximation theory: The basic theory for large language models, 2024a. URL <https://arxiv.org/abs/2407.00958>.
- Wei Wang and Qing Li. Universal approximation theory: Foundations for parallelism in neural networks, 2024b. URL <https://arxiv.org/abs/2407.21670>.
- Xintao Wang, Kelvin CK Chan, Ke Yu, Chao Dong, and Chen Change Loy. Edvr: Video restoration with enhanced deformable convolutional networks. In *Proceedings of the IEEE/CVF conference on computer vision and pattern recognition workshops*, pp. 0–0, 2019b.

-
- Zeyu Wang, Yutong Bai, Yuyin Zhou, and Cihang Xie. Can cnns be more robust than transformers? *ArXiv*, abs/2206.03452, 2022b. URL <https://api.semanticscholar.org/CorpusID:249431433>.
- Xiu-Shen Wei, Jian-Hao Luo, Jianxin Wu, and Zhi-Hua Zhou. Selective convolutional descriptor aggregation for fine-grained image retrieval. *IEEE Transactions on Image Processing*, 26:2868–2881, 2016. URL <https://api.semanticscholar.org/CorpusID:9557727>.
- Saining Xie, Ross B. Girshick, Piotr Dollár, Zhuowen Tu, and Kaiming He. Aggregated residual transformations for deep neural networks. *2017 IEEE Conference on Computer Vision and Pattern Recognition (CVPR)*, pp. 5987–5995, 2016. URL <https://api.semanticscholar.org/CorpusID:8485068>.
- Zhi-Qin John Xu, Yaoyu Zhang, and Yanyang Xiao. Training behavior of deep neural network in frequency domain. In *Neural Information Processing: 26th International Conference, ICONIP 2019, Sydney, NSW, Australia, December 12–15, 2019, Proceedings, Part I 26*, pp. 264–274. Springer, 2019.
- Yunfei Yang, Han Feng, and Ding-Xuan Zhou. On the rates of convergence for learning with convolutional neural networks. *ArXiv*, abs/2403.16459, 2024. URL <https://api.semanticscholar.org/CorpusID:268680734>.
- Dong Yin, Raphael Gontijo Lopes, Jon Shlens, Ekin Dogus Cubuk, and Justin Gilmer. A fourier perspective on model robustness in computer vision. *Advances in Neural Information Processing Systems*, 32, 2019.
- Ding-Xuan Zhou. Universality of deep convolutional neural networks. *ArXiv*, abs/1805.10769, 2018. URL <https://api.semanticscholar.org/CorpusID:44113176>.
- Ding-Xuan Zhou. Theory of deep convolutional neural networks: Downsampling. *Neural networks : the official journal of the International Neural Network Society*, 124:319–327, 2020. URL <https://api.semanticscholar.org/CorpusID:211070716>.

A THE UAT FORMAT OF RESIDUAL-BASED CNNs AND TRANSFORMER-BASED ViTs

Note: The sections A.1, Section A.2 and A.4 have already been proven in DUAT2LLMs. We also include them in this paper to ensure completeness.

In this section, we will show the DUAT mathematical form corresponding to residual-based CNNs and Transformer-based ViTs (which also use residual connections by design). In Section A.1, we first introduce a lemma concerning UAT and then we introduce the DUAT in Section A.2. Based on Section A.2, we show that both residual-based CNNs (see Section A.3) and Transformer-based ViTs (see Section A.4) are DUAT functions.

It is important to highlight that DUAT’s overall mathematical structure is aligned with UAT; the key distinction is that DUAT’s parameters are influenced by the input. Currently, this influence is achieved primarily through the use of residual connections. Therefore, we represent multi-layer residual networks in the corresponding UAT form and illustrate how their parameters are influenced by the input, establishing them as DUAT functions. Due to the close relationship between UAT and DUAT, some interchange of the terms UAT and DUAT may occur in the following sections.

A.1 THE PROPERTIES OF UAT

Before expressing residual-based CNNs and Transformer-based ViTs in the UAT format, we present a lemma regarding UAT. There are two cases for UAT-approximated functions: $f(\mathbf{x}) \in \mathbb{R}$ and $f(\mathbf{x}) \in \mathbb{R}^m$. The proof for the case where $f(\mathbf{x}) \in \mathbb{R}$ can be inferred from $f(\mathbf{x}) \in \mathbb{R}^m$. Therefore, we will only provide the proof for approximating $f(\mathbf{x}) \in \mathbb{R}^m$ using UAT.

Lemma 1. The mathematical form of UAT remains unchanged when multiplied by a matrix (constant).

$$\begin{aligned} G(\mathbf{x}) &= \beta \sum_{j=1}^N \alpha_j \sigma(\mathbf{W}_j^T \mathbf{x} + \theta_j) \\ &= \sum_{j=1}^N \beta \alpha_j \sigma(\mathbf{W}_j^T \mathbf{x} + \theta_j) \end{aligned} \tag{7}$$

Eq. 7 shows the representation of UAT multiplying a matrix. Let $\alpha_j = \beta \alpha_j$, and the general mathematical form of Eq. 7 remains consistent with the original UAT mathematical form. Thus, it is proven that the mathematical form of UAT remains unchanged when multiplied by a matrix (constant).

A.2 FROM UAT TO DUAT

In this section, we first present a general form for a single-layer residual term in a network and demonstrate that the mathematical form of a multi-layer network composed of this residual term aligns with the DUAT framework. Before proceeding with the formal proof, we first define DUAT explicitly: DUAT shares the overall mathematical form of UAT, but with certain parameters influenced by the input, allowing them to change dynamically in response to it. We refer to these parameters as ”dynamic parameters.” In standard UAT, parameters remain fixed once training is complete, whereas, in DUAT, the dynamic parameters are functions of the input and thus vary with it. Consequently, dynamic parameters in DUAT may take the form of complex functions. Currently, DUAT primarily is implemented by residual structure, meaning that, in general, these complex functions are also DUAT. Next, we will give the proof.

A general residual term of the network can be written as:

$$\mathbf{x}'_i = (\mathbf{W}'_{i,1} \mathbf{x}'_{i-1} + \mathbf{b}'_{i,3}) + \mathbf{W}'_{i,3} \sigma(\mathbf{W}'_{i,2} \mathbf{x}'_{i-1} + \mathbf{b}'_{i,2}) \tag{8}$$

where $i = 1, 2, 3, \dots$ and \mathbf{x}'_0 represents the input. A multi-layer network structured in this way aligns with the mathematical form of DUAT. To demonstrate that a multi-layer network leverages

the general term of Eq. 8 corresponds to DUAT, we first examine the forms of single-layer and two-layer networks, as shown in Eqs. 9 and 10.

$$\mathbf{x}'_1 = (\mathbf{W}'_{1,1}\mathbf{x}'_0 + \mathbf{b}'_{1,3}) + \mathbf{W}'_{1,3}\sigma(\mathbf{W}'_{1,2}\mathbf{x}'_0 + \mathbf{b}'_{1,2}) \quad (9)$$

$$\begin{aligned} \mathbf{x}'_2 &= \mathbf{W}'_{2,1}\mathbf{x}'_1 + \mathbf{W}'_{2,3}\sigma(\mathbf{W}'_{2,2}\mathbf{x}'_1 + \mathbf{b}'_{2,2}) + \mathbf{b}'_{2,3} \\ &= (\mathbf{W}'_{2,1}\mathbf{x}'_1 + \mathbf{b}'_{2,3}) + \mathbf{W}'_{2,3}\sigma(\mathbf{W}'_{2,2}\mathbf{x}'_1 + \mathbf{b}'_{2,2}) \\ &= \{\mathbf{W}'_{2,1}[(\mathbf{W}'_{1,1}\mathbf{x}'_0 + \mathbf{b}'_{1,3}) + \mathbf{W}'_{1,3}\sigma(\mathbf{W}'_{1,2}\mathbf{x}'_0 + \mathbf{b}'_{1,2})] + \mathbf{b}'_{2,3}\} \\ &\quad + \mathbf{W}'_{2,3}\sigma\{\mathbf{W}'_{2,2}[(\mathbf{W}'_{1,1}\mathbf{x}'_0 + \mathbf{b}'_{1,3}) + \mathbf{W}'_{1,3}\sigma(\mathbf{W}'_{1,2}\mathbf{x}'_0 + \mathbf{b}'_{1,2})] + \mathbf{b}'_{2,2}\} \\ &= \{\mathbf{W}'_{2,1}(\mathbf{W}'_{1,1}\mathbf{x}'_0 + \mathbf{b}'_{1,3}) + \mathbf{b}'_{2,3} + \mathbf{W}'_{2,1}\mathbf{W}'_{1,3}\sigma(\mathbf{W}'_{1,2}\mathbf{x}'_0 + \mathbf{b}'_{1,2})\} \\ &\quad + \mathbf{W}'_{2,3}\sigma\{\mathbf{W}'_{2,2}(\mathbf{W}'_{1,1}\mathbf{x}'_0 + \mathbf{b}'_{1,3}) + \mathbf{b}'_{2,2} + \mathbf{W}'_{2,2}\mathbf{W}'_{1,3}\sigma(\mathbf{W}'_{1,2}\mathbf{x}'_0 + \mathbf{b}'_{1,2})\} \\ &= \{(\mathbf{W}'_{2,1}\mathbf{W}'_{1,1}\mathbf{x}'_0 + \mathbf{W}'_{2,1}\mathbf{b}'_{1,3} + \mathbf{b}'_{2,3}) + \mathbf{W}'_{2,1}\mathbf{W}'_{1,3}\sigma(\mathbf{W}'_{1,2}\mathbf{x}'_0 + \mathbf{b}'_{1,2})\} \\ &\quad + \mathbf{W}'_{2,3}\sigma\{\mathbf{W}'_{2,2}\mathbf{W}'_{1,1}\mathbf{x}'_0 + (\mathbf{W}'_{2,2}\mathbf{b}'_{1,3} + \mathbf{b}'_{2,2}) + \mathbf{W}'_{2,2}\mathbf{W}'_{1,3}\sigma(\mathbf{W}'_{1,2}\mathbf{x}'_0 + \mathbf{b}'_{1,2})\} \end{aligned} \quad (10)$$

In Eq. 10, let $\mathbf{W}'_{2,1} = \mathbf{W}'_{2,1}\mathbf{W}'_{1,1}$, $\mathbf{b}'_{2,1} = \mathbf{W}'_{2,1}\mathbf{b}'_{1,3} + \mathbf{b}'_{2,3}$, $\mathbf{W}'_{1,3} = \mathbf{W}'_{2,1}\mathbf{W}'_{1,3}$, $\mathbf{W}'_{2,2} = \mathbf{W}'_{2,2}\mathbf{W}'_{1,1}$, and $\mathbf{b}'_{2,2} = (\mathbf{W}'_{2,2}\mathbf{b}'_{1,3} + \mathbf{b}'_{2,2}) + \mathbf{W}'_{2,2}\mathbf{W}'_{1,3}\sigma(\mathbf{W}'_{1,2}\mathbf{x}'_0 + \mathbf{b}'_{1,2})$. Thus, Eq. 10 can be written into Eq. 11.

$$\begin{aligned} \mathbf{x}'_2 &= (\mathbf{W}'_{2,1}\mathbf{x}'_0 + \mathbf{b}'_{2,1}) + \mathbf{W}'_{1,3}\sigma(\mathbf{W}'_{1,2}\mathbf{x}'_0 + \mathbf{b}'_{1,2}) \\ &\quad + \mathbf{W}'_{2,3}\sigma(\mathbf{W}'_{2,2}\mathbf{x}'_0 + \mathbf{b}'_{2,2}) \end{aligned} \quad (11)$$

For the clarity, we could write Eq. 9 and Eq. 11 into Eq. 12 and Eq. 13, where $UAT_1^R = \mathbf{W}'_{1,3}\sigma(\mathbf{W}'_{1,2}\mathbf{x}'_0 + \mathbf{b}'_{1,2})$ and $UAT_2^R = \sum_{j=1}^2 \mathbf{W}'_{j,3}\sigma(\mathbf{W}'_{j,2}\mathbf{x}'_0 + \mathbf{b}'_{j,2})$.

$$\mathbf{x}'_1 = (\mathbf{W}'_{1,1}\mathbf{x}'_0 + \mathbf{b}'_{1,3}) + UAT_1^R \quad (12)$$

$$\mathbf{x}'_2 = (\mathbf{W}'_{2,1}\mathbf{x}'_0 + \mathbf{b}'_{2,1}) + UAT_2^R \quad (13)$$

According to Eq. 12 and Eq. 13, aside from the initial term, the overall mathematical forms of the residual terms UAT_1^R and UAT_2^R are consistent with UAT. However, for UAT_2^R , its parameter $\mathbf{b}'_{2,2}$ is influenced by the input, while other weight parameters, such as $\mathbf{W}'_{2,1}$, can be disregarded. These parameters are only affected by other parameters, so once the network training is complete, they are essentially fixed. This allows us to focus primarily on the dynamic parameters. In Eq. $\mathbf{b}'_{2,2} = (\mathbf{W}'_{2,2}\mathbf{b}'_{1,3} + \mathbf{b}'_{2,2}) + \mathbf{W}'_{2,2}\mathbf{W}'_{1,3}\sigma(\mathbf{W}'_{1,2}\mathbf{x}'_0 + \mathbf{b}'_{1,2})$, except for the initial term, $\mathbf{b}'_{2,2}$ also follows the same mathematical form as UAT. This can be interpreted as dynamically adjusting the bias term $\mathbf{b}'_{2,2}$ via UAT based on the input. In conclusion, we have demonstrated that the mathematical forms of one-layer and two-layer residual networks are consistent with the UAT framework and the two-layer residual network is the DUAT function.

Next, we will use mathematical induction to prove that the mathematical form of a multi-layer residual network is also a DUAT function. Assume that the overall mathematical form of the first i layers of the residual network aligns with UAT. Our goal is to show that the overall mathematical form of the $i + 1$ -th layer remains consistent with UAT.

For clarity, we make the following definitions: since the overall mathematical form of the first i layers is consistent with UAT, we can write it as $\mathbf{x}'_i = (\mathbf{W}'_{i,1}\mathbf{x}'_0 + \mathbf{b}'_{i,1}) + UAT_i^R$, where the first term is explicitly written, and the remainder is denoted as UAT_i^R , with $UAT_i^R = \sum_{j=1}^i \mathbf{W}'_{j,3}\sigma(\mathbf{W}'_{j,2}\mathbf{x}'_0 + \mathbf{b}'_{j,2})$. Since $\mathbf{x}'_{i+1} = (\mathbf{W}'_{i+1,1}\mathbf{x}'_i + \mathbf{b}'_{i+1,3}) + \mathbf{W}'_{i+1,3}\sigma(\mathbf{W}'_{i+1,2}\mathbf{x}'_i + \mathbf{b}'_{i+1,2})$, we divide \mathbf{x}'_{i+1} into two parts: $(\mathbf{W}'_{i+1,1}\mathbf{x}'_i + \mathbf{b}'_{i+1,3})$ and $\mathbf{W}'_{i+1,3}\sigma(\mathbf{W}'_{i+1,2}\mathbf{x}'_i + \mathbf{b}'_{i+1,2})$.

First, consider $(\mathbf{W}'_{i+1,1}\mathbf{x}'_i + \mathbf{b}'_{i+1,3})$. Substituting $\mathbf{x}'_i = (\mathbf{W}'_{i,1}\mathbf{x}'_0 + \mathbf{b}'_{i,1}) + UAT_i^R$, we obtain Eq. 14. Setting $\mathbf{W}'_{i+1,1} = \mathbf{W}'_{i+1,1}\mathbf{W}'_{i,1}$ and $\mathbf{b}'_{i+1,1} = \mathbf{W}'_{i+1,1}\mathbf{b}'_{i,1} + \mathbf{b}'_{i+1,3}$, we can simplify the first part to $(\mathbf{W}'_{i+1,1}\mathbf{x}'_0 + \mathbf{b}'_{i+1,1}) + \mathbf{W}'_{i+1,1}UAT_i^R$. Since the overall mathematical form of UAT_i^R is consistent with the i -layer UAT and we have shown that the UAT form is preserved when multiplied by a matrix, we have thus demonstrated that the overall mathematical form of the first part remains consistent with UAT.

$$\begin{aligned}
& (\mathbf{W}'_{i+1,1}\mathbf{x}'_i + \mathbf{b}'_{i+1,3}) \\
&= \{\mathbf{W}'_{i+1,1}[(\mathbf{W}'_{i,1}\mathbf{x}'_0 + \mathbf{b}'_{i,1}) + UAT_i^R] + \mathbf{b}'_{i+1,3}\} \\
&= \{\mathbf{W}'_{i+1,1}(\mathbf{W}'_{i,1}\mathbf{x}'_0 + \mathbf{b}'_{i,1}) + \mathbf{W}'_{i+1,1}UAT_i^R + \mathbf{b}'_{i+1,3}\} \\
&= \{[\mathbf{W}'_{i+1,1}\mathbf{W}'_{i,1}\mathbf{x}'_0 + (\mathbf{W}'_{i+1,1}\mathbf{b}'_{i,1} + \mathbf{b}'_{i+1,3})] + \mathbf{W}'_{i+1,1}UAT_i^R\}
\end{aligned} \tag{14}$$

Next, we show that the overall mathematical form of the second part, $\mathbf{W}'_{i+1,3}\sigma(\mathbf{W}'_{i+1,2}\mathbf{x}'_i + \mathbf{b}'_{i+1,2})$, is also consistent with UAT. Substituting $\mathbf{x}'_i = (\mathbf{W}'_{i,1}\mathbf{x}'_0 + \mathbf{b}'_{i,1}) + UAT_i^R$ into this expression, we arrive at Eq. 15. Setting $\mathbf{W}'_{i+1,2} = \mathbf{W}'_{i+1,2}\mathbf{W}'_{i,1}$ and $\mathbf{b}'_{i+1,2} = (\mathbf{W}'_{i+1,2}\mathbf{b}'_{i,1} + \mathbf{b}'_{i+1,2}) + \mathbf{W}'_{i+1,2}UAT_i^R$, we can rewrite the second part as $\mathbf{W}'_{i+1,3}\sigma(\mathbf{W}'_{i+1,2}\mathbf{x}'_0 + \mathbf{b}'_{i+1,2})$, which can be interpreted as a term in UAT. Here, $\mathbf{b}'_{i+1,2}$ serves as a bias term approximated using DUAT.

$$\begin{aligned}
& \mathbf{W}'_{i+1,3}\sigma(\mathbf{W}'_{i+1,2}\mathbf{x}'_i + \mathbf{b}'_{i+1,2}) \\
&= \mathbf{W}'_{i+1,3}\sigma\{\mathbf{W}'_{i+1,2}[(\mathbf{W}'_{i,1}\mathbf{x}'_0 + \mathbf{b}'_{i,1}) + UAT_i^R] + \mathbf{b}'_{i+1,2}\} \\
&= \mathbf{W}'_{i+1,3}\sigma\{\mathbf{W}'_{i+1,2}(\mathbf{W}'_{i,1}\mathbf{x}'_0 + \mathbf{b}'_{i,1}) + \mathbf{W}'_{i+1,2}UAT_i^R + \mathbf{b}'_{i+1,2}\} \\
&= \mathbf{W}'_{i+1,3}\sigma\{\mathbf{W}'_{i+1,2}\mathbf{W}'_{i,1}\mathbf{x}'_0 + (\mathbf{W}'_{i+1,2}\mathbf{b}'_{i,1} + \mathbf{b}'_{i+1,2}) + \mathbf{W}'_{i+1,2}UAT_i^R\}
\end{aligned} \tag{15}$$

Let $UAT_{i+1}^R = \mathbf{W}'_{i+1,1}UAT_i^R + \mathbf{W}'_{i+1,3}\sigma(\mathbf{W}'_{i+1,2}\mathbf{x}'_0 + \mathbf{b}'_{i+1,2})$. Then, we can express \mathbf{x}'_{i+1} as $\mathbf{x}'_{i+1} = (\mathbf{W}'_{i+1,1}\mathbf{x}'_0 + \mathbf{b}'_{i+1,1}) + UAT_{i+1}^R$. Thus, apart from the initial term, the overall mathematical form of \mathbf{x}'_{i+1} remains consistent with UAT. Since a single term does not alter the nature of UAT, we conclude that the overall form of a multi-layer residual network aligns with UAT. Furthermore, as certain bias parameters within the network, such as $\mathbf{b}'_{i+1,2}$, are also approximated using UAT, we have therefore demonstrated that the mathematical form of a multi-layer residual network is a UAT function.

A.3 THE DUAT FORMAT OF RESIDUAL-BASED CNNs

To demonstrate that the residual-based CNN is indeed a DUAT function, we present its general form as defined by Figure 8 in the main text, represented by Eq. 16. Comparing this with the general form provided in Section A.2, specifically $\mathbf{x}'_{i+1} = (\mathbf{W}'_{i+1,1}\mathbf{x}'_i + \mathbf{b}'_{i+1,3}) + \mathbf{W}'_{i+1,3}\sigma(\mathbf{W}'_{i+1,2}\mathbf{x}'_i + \mathbf{b}'_{i+1,2})$, we find their only distinction lies in the term $\mathbf{W}'_{i+1,1}\mathbf{x}'_i + \mathbf{b}'_{i+1,3}$. It is straightforward to deduce that the presence or absence of $\mathbf{W}'_{i+1,1}$ does not affect the overall mathematical form. Therefore, the residual-based CNN also qualifies as a DUAT function.

$$\begin{aligned}
\mathbf{x}'_{i+1} &= \mathbf{x}'_i + \mathbf{W}'_{i+1,2}\sigma(\mathbf{W}'_{i+1,1}\mathbf{x}'_i + \mathbf{b}_{i+1,1}) + \mathbf{b}'_{i+1,2} \\
&= (\mathbf{x}'_i + \mathbf{b}'_{i+1,2}) + \mathbf{W}'_{i+1,2}\sigma(\mathbf{W}'_{i+1,1}\mathbf{x}'_i + \mathbf{b}'_{i+1,1})
\end{aligned} \tag{16}$$

To clearly present the DUAT form of residual-based CNNs, we apply the method described in Section A.2. Assuming that the general mathematical form of \mathbf{x}'_i aligns with UAT, we decompose \mathbf{x}'_i into a primary term and a remainder term, expressed as $\mathbf{x}'_i = (\mathbf{x}'_0 + \mathbf{b}'_{i,2}) + UAT_i^R$, where $UAT_i^R = \sum_{j=1}^i \mathbf{W}'_{j,2}\sigma(\mathbf{W}'_{j,1}\mathbf{x}'_0 + \mathbf{b}'_{j,1})$ for $i \geq 1$. Substituting this into $\mathbf{x}'_{i+1} = (\mathbf{x}'_i + \mathbf{b}'_{i+1,2}) + \mathbf{W}'_{i+1,2}\sigma(\mathbf{W}'_{i+1,1}\mathbf{x}'_i + \mathbf{b}'_{i+1,1})$, we derive Eq. 18.

By setting $\mathbf{b}'_{i+1,2} = \mathbf{b}'_{i,2} + \mathbf{b}'_{i+1,2}$ and $\mathbf{b}'_{i+1,1} = (\mathbf{W}'_{i+1,1}\mathbf{b}'_{i,1} + \mathbf{b}'_{i+1,1}) + \mathbf{W}'_{i+1,1}UAT_i^R$, we obtain $\mathbf{x}'_{i+1} = (\mathbf{x}'_0 + \mathbf{b}'_{i+1,2}) + UAT_i^R + \mathbf{W}'_{i+1,2}\sigma(\mathbf{W}'_{i+1,1}\mathbf{x}'_0 + \mathbf{b}'_{i+1,1})$. Given that the overall mathematical format of UAT_i^R is consistent with the UAT formula, it follows that \mathbf{x}'_{i+1} also conforms to the UAT format.

Furthermore, we define $UAT_{i+1}^R = UAT_i^R + \mathbf{W}'_{i+1,2}\sigma(\mathbf{W}'_{i+1,1}\mathbf{x}'_0 + \mathbf{b}'_{i+1,1})$, leading to $\mathbf{x}'_{i+1} = (\mathbf{x}'_0 + \mathbf{b}'_{i+1,2}) + UAT_{i+1}^R$, where $UAT_{i+1}^R = \sum_{j=1}^{i+1} \mathbf{W}'_{j,2}\sigma(\mathbf{W}'_{j,1}\mathbf{x}'_0 + \mathbf{b}'_{j,1})$. Thus, $i + 1$ -layer residual-based CNN is:

$$\mathbf{x}'_{i+1} = (\mathbf{x}'_0 + \mathbf{b}'_{i+1,2}) + \sum_{j=1}^{i+1} \mathbf{W}'_{j,2}\sigma(\mathbf{W}'_{j,1}\mathbf{x}'_0 + \mathbf{b}'_{j,1}) \quad (17)$$

where $i = 0, 1, 2, \dots$. For $i = 0$, we have $\mathbf{b}'_{1,1} = \mathbf{b}'_{1,1}$; and for $i > 0$, $\mathbf{b}'_{j,1}$ is defined by $\mathbf{b}'_{j,1} = (\mathbf{W}'_{j,1}\mathbf{b}'_{j-1,2} + \mathbf{b}'_{j,1}) + \mathbf{W}'_{j,1}\sum_{k=1}^{j-1} \mathbf{W}'_{k,2}\sigma(\mathbf{W}'_{k,1}\mathbf{x}'_0 + \mathbf{b}'_{k,1})$. Thus, $\mathbf{b}'_{j,1}$ can be seen as a j -layer UAT and the input is \mathbf{x}'_0 . For convenience, we also consider the first term as part of the UAT. Additionally, for the term $\mathbf{b}'_{j+1,2}$ at layer i , it is given by $\mathbf{b}'_{j+1,2} = \mathbf{b}'_{1,2} \cdots \mathbf{b}'_{j,2} + \mathbf{b}'_{j+1,2}$, $j = 1, 2 \cdots i$. Naturally, in a multilayer network, $\mathbf{b}'_{i,2}$, $i \geq 1$ within the corresponding UAT will also change. However, as shown in the derivation above, these adjustments involve only matrix addition of predefined parameters. Therefore, they can essentially be understood as fixed parameters and do not fundamentally alter the mathematical form of the UAT. Consequently, we will not elaborate on the specific forms of these parameters here. Some examples are provided in Figure 11. Since $\mathbf{b}'_{j,1}$ adapts dynamically to the input, the multilayer convolutional network based on residuals can essentially be understood as a DUAT function.

$$\begin{aligned} & (\mathbf{x}'_i + \mathbf{b}_{i+1,2}) + \mathbf{W}'_{i+1,2}\sigma(\mathbf{W}'_{i+1,1}\mathbf{x}'_i + \mathbf{b}_{i+1,1}) \\ &= [(\mathbf{x}_0 + \mathbf{b}_{i,1}) + UAT_i^R + \mathbf{b}_{i+1,2}] + \mathbf{W}'_{i+1,2}\sigma\{\mathbf{W}'_{i+1,1}[(\mathbf{x}_0 + \mathbf{b}_{i,1}) + UAT_i^R] + \mathbf{b}_{i+1,1}\} \\ &= (\mathbf{x}_0 + \mathbf{b}_{i,1} + \mathbf{b}_{i+1,2}) + UAT_i^R + \mathbf{W}'_{i+1,2}\sigma\{\mathbf{W}'_{i+1,1}\mathbf{x}_0 + \underbrace{(\mathbf{W}'_{i+1,1}\mathbf{b}_{i,1} + \mathbf{b}_{i+1,1})}_{UAT_i^R} + \mathbf{W}'_{i+1,1}UAT_i^R\} \end{aligned} \quad (18)$$

$\mathbf{x}'_1 = (\mathbf{x}'_0 + \mathbf{b}_{1,2}) + \mathbf{W}'_{1,2}\sigma(\mathbf{W}'_{1,1}\mathbf{x}'_0 + \mathbf{b}_{1,1})$	$\mathbf{x}'_1 = (\mathbf{x}'_0 + \mathbf{b}_{1,2}) + UAT_1^R$	$UAT_1^R = \mathbf{W}'_{1,2}\sigma(\mathbf{W}'_{1,1}\mathbf{x}'_0 + \mathbf{b}_{1,1})$
$\mathbf{x}'_2 = (\mathbf{x}'_0 + \mathbf{b}_{2,2}) + \mathbf{W}'_{1,2}\sigma(\mathbf{W}'_{1,1}\mathbf{x}'_0 + \mathbf{b}_{1,1})$ $+ \mathbf{W}'_{2,2}\sigma(\mathbf{W}'_{2,1}\mathbf{x}'_0 + \mathbf{b}_{2,1})$ <hr style="border-top: 1px dashed black;"/> $\mathbf{b}_{2,2} = \mathbf{b}_{1,2} + \mathbf{b}_{2,2}$ $\mathbf{b}_{2,1} = (\mathbf{W}'_{2,1}\mathbf{b}_{1,2} + \mathbf{b}_{2,1}) + \mathbf{W}'_{2,1}\mathbf{W}'_{1,2}\sigma(\mathbf{W}'_{1,1}\mathbf{x}'_0 + \mathbf{b}_{1,1})$	$\mathbf{x}'_2 = (\mathbf{x}'_0 + \mathbf{b}_{2,2}) + UAT_2^R$	$UAT_2^R = \mathbf{W}'_{1,2}\sigma(\mathbf{W}'_{1,1}\mathbf{x}'_0 + \mathbf{b}_{1,1})$ $+ \mathbf{W}'_{2,2}\sigma(\mathbf{W}'_{2,1}\mathbf{x}'_0 + \mathbf{b}_{2,1})$
$\mathbf{x}'_3 = (\mathbf{x}'_0 + \mathbf{b}_{3,2}) + \mathbf{W}'_{1,2}\sigma(\mathbf{W}'_{1,1}\mathbf{x}'_0 + \mathbf{b}_{1,1})$ $+ \mathbf{W}'_{2,2}\sigma(\mathbf{W}'_{2,1}\mathbf{x}'_0 + \mathbf{b}_{2,1}) + \mathbf{W}'_{3,2}\sigma(\mathbf{W}'_{3,1}\mathbf{x}'_0 + \mathbf{b}_{3,1})$ <hr style="border-top: 1px dashed black;"/> $\mathbf{b}_{3,2} = \mathbf{b}_{2,2} + \mathbf{b}_{3,2}$ $\mathbf{b}_{3,1} = (\mathbf{W}'_{3,1}\mathbf{b}_{2,2} + \mathbf{b}_{3,1}) + \mathbf{W}'_{3,1}\mathbf{W}'_{1,2}\sigma(\mathbf{W}'_{1,1}\mathbf{x}'_0 + \mathbf{b}_{1,1})$ $+ \mathbf{W}'_{3,1}\mathbf{W}'_{2,2}\sigma(\mathbf{W}'_{2,1}\mathbf{x}'_0 + \mathbf{b}_{2,1})$	$\mathbf{x}'_3 = (\mathbf{x}'_0 + \mathbf{b}_{3,2}) + UAT_3^R$	$UAT_3^R = \mathbf{W}'_{1,2}\sigma(\mathbf{W}'_{1,1}\mathbf{x}'_0 + \mathbf{b}_{1,1})$ $+ \mathbf{W}'_{2,2}\sigma(\mathbf{W}'_{2,1}\mathbf{x}'_0 + \mathbf{b}_{2,1})$ $+ \mathbf{W}'_{3,2}\sigma(\mathbf{W}'_{3,1}\mathbf{x}'_0 + \mathbf{b}_{3,1})$
\vdots	\vdots	\vdots

Figure 11: Some examples of the UAT format of multi-layer residual-based convolution. The changes of parameters are represented within the dashed boxes. The parameters on the right of the equations indicate the original values, while those on the left represent the transformed values. There is no specific order of calculation for the parameters within each dashed box, but there is a top-to-bottom calculation order between different dashed boxes.

A.4 THE DUAT FORMAT OF TRANSFORMER-BASED ViTs

Similarly, to prove that Transformer-based ViTs are also DUAT functions, we start by deriving their general form based on Figure 9 in the main text. Transformers involve two key operations: Multi-Head Attention (MHA) and the Feed-Forward Network (FFN). In matrix-vector form, these operations correspond to Eqs. 19 and 20.

$$MHA(\mathbf{x}_i) \mapsto \mathbf{W}'_{i,1}\mathbf{x}'_i \quad (19)$$

$$FFN(\mathbf{x}_i) \mapsto \mathbf{W}'_{i,3}\sigma(\mathbf{W}'_{i,2}\mathbf{x}'_i + \mathbf{b}'_{i,2}) + \mathbf{b}'_{i,3} \quad (20)$$

$$\begin{aligned} \mathbf{x}'_{i+1} &= \mathbf{W}'_{i+1,1}\mathbf{x}'_i + \mathbf{W}'_{i+1,3}\sigma[\mathbf{W}'_{i+1,2}(\mathbf{W}'_{i+1,1}\mathbf{x}'_i) + \mathbf{b}'_{i+1,2}] + \mathbf{b}'_{i+1,3} \\ &= \mathbf{W}'_{i+1,1}\mathbf{x}'_i + \mathbf{W}'_{i+1,3}\sigma(\mathbf{W}'_{i+1,2}\mathbf{W}'_{i+1,1}\mathbf{x}'_i + \mathbf{b}'_{i+1,2}) + \mathbf{b}'_{i+1,3} \end{aligned} \quad (21)$$

Thus, a general term in a Transformer-based network can be expressed as Eq. 21. Letting $\mathbf{W}'_{i+1,2} = \mathbf{W}'_{i+1,2}\mathbf{W}'_{i+1,1}$, we can rewrite the general term as follows:

$$\mathbf{x}'_{i+1} = (\mathbf{W}'_{i+1,1}\mathbf{x}'_i + \mathbf{b}'_{i+1,3}) + \mathbf{W}'_{i,3}\sigma(\mathbf{W}'_{i+1,2}\mathbf{x}'_i + \mathbf{b}'_{i+1,2}) \quad (22)$$

Clearly, Eq. 22 matches the mathematical form presented in Section A.2: $\mathbf{x}'_{i+1} = (\mathbf{W}'_{i+1,1}\mathbf{x}'_i + \mathbf{b}'_{i+1,3}) + \mathbf{W}'_{i+1,3}\sigma(\mathbf{W}'_{i+1,2}\mathbf{x}'_i + \mathbf{b}'_{i+1,2})$. Therefore, a multilayer Transformer-based ViT is indeed DUAT function.

To clearly show the DUAT format of a multilayer ViT, we use the approach outlined in Section A.2. Assuming that the overall mathematical form of \mathbf{x}'_i aligns with the UAT structure, we decompose \mathbf{x}'_i into a main term and a residual term, expressed as $\mathbf{x}'_i = (\mathbf{W}_{i,1}\mathbf{x}_0 + \mathbf{b}_{i,3}) + UAT_i^R$, where $UAT_i^R = \sum_{j=1}^i \mathbf{W}'_{j,3}\sigma(\mathbf{W}'_{j,2}\mathbf{x}'_0 + \mathbf{b}'_{j,2})$ and $i = 1, 2, \dots$. Substituting this into $\mathbf{x}'_{i+1} = (\mathbf{W}'_{i+1,1}\mathbf{x}'_i + \mathbf{b}'_{i+1,3}) + \mathbf{W}'_{i,3}\sigma(\mathbf{W}'_{i+1,2}\mathbf{x}'_i + \mathbf{b}'_{i+1,2})$, we get Eq. 23.

$$\begin{aligned} \mathbf{x}'_{i+1} &= (\mathbf{W}'_{i+1,1}\mathbf{x}'_i + \mathbf{b}'_{i+1,3}) + \mathbf{W}'_{i,3}\sigma(\mathbf{W}'_{i+1,2}\mathbf{x}'_i + \mathbf{b}'_{i+1,2}) \\ &= \{\mathbf{W}'_{i+1,1}[(\mathbf{W}_{i,1}\mathbf{x}_0 + \mathbf{b}_{i,1}) + UAT_i^R] + \mathbf{b}'_{i+1,3}\} \\ &\quad + \mathbf{W}'_{i,3}\sigma\{\mathbf{W}'_{i+1,2}[(\mathbf{W}_{i,1}\mathbf{x}_0 + \mathbf{b}_{i,1}) + UAT_i^R] + \mathbf{b}'_{i+1,2}\} \\ &= [\mathbf{W}'_{i+1,1}\mathbf{W}_{i,1}\mathbf{x}_0 + (\mathbf{W}'_{i+1,1}\mathbf{b}_{i,1} + \mathbf{b}'_{i+1,3})] + \mathbf{W}'_{i+1,1}UAT_i^R \\ &\quad + \mathbf{W}'_{i,3}\sigma\{\mathbf{W}'_{i+1,2}\mathbf{W}_{i,1}\mathbf{x}_0 + (\mathbf{W}'_{i+1,2}\mathbf{b}_{i,1} + \mathbf{b}'_{i+1,2}) + \mathbf{W}'_{i+1,2}UAT_i^R\} \end{aligned} \quad (23)$$

Let $\mathbf{W}'_{i+1,1} = \mathbf{W}'_{i+1,1}\mathbf{W}_{i,1}$, $\mathbf{b}'_{i+1,3} = (\mathbf{W}'_{i+1,1}\mathbf{b}_{i,1} + \mathbf{b}'_{i+1,3})$, $UAT_i^R = \mathbf{W}'_{i+1,1}UAT_i^R$, $\mathbf{W}'_{i+1,2} = \mathbf{W}'_{i+1,2}\mathbf{W}_{i,1}$, and $\mathbf{b}'_{i+1,2} = (\mathbf{W}'_{i+1,2}\mathbf{b}_{i,1} + \mathbf{b}'_{i+1,2}) + \mathbf{W}'_{i+1,2}UAT_i^R$. Substituting these, we obtain $\mathbf{x}'_{i+1} = (\mathbf{W}'_{i+1,1}\mathbf{x}_0 + \mathbf{b}'_{i+1,3}) + UAT_i^R + \mathbf{W}'_{i,3}\sigma(\mathbf{W}'_{i+1,2}\mathbf{x}_0 + \mathbf{b}'_{i+1,2})$. Since UAT_i^R overall aligns with the UAT, the overall mathematical form of the $i + 1$ layers' ViT also conforms to the UAT.

So the $i + 1$ layers' ViT can be expressed as:

$$\mathbf{x}_{i+1} = (\mathbf{W}'_{i+1,1}\mathbf{x}_0 + \mathbf{b}_{i+1,3}) + \sum_{j=1}^{i+1} \mathbf{W}'_{j,3}\sigma(\mathbf{W}'_{j,2}\mathbf{x}'_0 + \mathbf{b}'_{j,2}) \quad (24)$$

When $i = 0$, the parameters are defined as follows: $\mathbf{W}'_{1,1} = \mathbf{W}'_{1,1}$, $\mathbf{b}'_{1,3} = \mathbf{b}'_{1,3}$, $\mathbf{W}'_{1,3} = \mathbf{W}'_{1,3}$, $\mathbf{W}'_{1,2} = \mathbf{W}'_{1,2}\mathbf{W}'_{1,1}$, and $\mathbf{b}'_{1,2} = \mathbf{b}'_{1,2}$. We define the parameters for cases where $i \geq 1$. For each

$j = 1, 2, \dots, i$, the updates are as follows: $\mathbf{W}'_{j+1,1} = \mathbf{W}'_{j+1,1} \mathbf{W}_{j,1}$, $\mathbf{b}'_{j+1,3} = \mathbf{W}'_{j+1,1} \mathbf{b}_{j,3} + \mathbf{b}'_{j+1,3}$, $\mathbf{W}'_{j+1,2} = \mathbf{W}'_{j+1,2} \mathbf{W}_{j,1}$, and $\mathbf{W}'_{j,3} = \mathbf{W}'_{j+1,1} \mathbf{W}'_{j,3}$.

Additionally, for $j = 1, 2, \dots, i + 1$, the bias terms $\mathbf{b}'_{j,2}$ are updated according to:

$$\begin{aligned} \mathbf{b}'_{j,2} = & (\mathbf{W}'_{j,2} \mathbf{b}'_{j-1,3} + \mathbf{b}'_{j,2}) \\ & + \mathbf{W}'_{j,2} \sum_{k=1}^{j-1} \mathbf{W}'_{k,3} \sigma(\mathbf{W}'_{k,2} \mathbf{x}'_0 + \mathbf{b}'_{k,2}). \end{aligned} \quad (25)$$

It means that the whole computing process is serial, if we want to compute $\mathbf{W}'_{3,1}$, we must calculate $\mathbf{W}'_{2,1}$, because $\mathbf{W}'_{3,1} = \mathbf{W}'_{3,1} \mathbf{W}'_{2,1}$. Thus, we have established that a multilayer ViT is also a DUAT function. The mathematical representation of the ViT aligns with the DUAT framework, with $\mathbf{b}'_{j,2}$ closely approximated by DUAT. The most notable difference between ViTs and residual-based CNNs is the dynamic input-dependent nature of the parameters in the MHA mechanism. Consequently, in the DUAT formulation associated with ViT, the parameters $\mathbf{W}'_{j,1}$ and $\mathbf{W}'_{j,2}$ for $i + 1 \geq j \geq 1$, and $\mathbf{W}'_{j,3}$ for $i + 1 > j > 1$ in layer i , all adapt dynamically based on the input.

$\mathbf{x}'_1 = (\mathbf{W}'_{1,1} \mathbf{x}'_0 + \mathbf{b}'_{1,3}) + \mathbf{W}'_{1,3} \sigma(\mathbf{W}'_{1,2} \mathbf{x}'_0 + \mathbf{b}'_{1,2})$ <div style="border: 1px dashed black; padding: 5px; margin: 5px 0;"> $\mathbf{W}'_{1,2} = \mathbf{W}'_{1,2} \mathbf{W}'_{1,1}$ </div>	$\mathbf{x}'_1 = (\mathbf{W}_{1,1} \mathbf{x}'_0 + \mathbf{b}_{1,3}) + UAT_1^R$	$UAT_1^R = \mathbf{W}'_{1,3} \sigma(\mathbf{W}'_{1,2} \mathbf{x}'_0 + \mathbf{b}'_{1,2})$
$\mathbf{x}'_2 = (\mathbf{W}'_{2,1} \mathbf{x}'_0 + \mathbf{b}'_{2,3}) + \mathbf{W}'_{1,3} \sigma(\mathbf{W}'_{1,2} \mathbf{x}'_0 + \mathbf{b}'_{1,2}) + \mathbf{W}'_{2,3} \sigma(\mathbf{W}'_{2,2} \mathbf{x}'_0 + \mathbf{b}'_{2,2})$ <div style="border: 1px dashed black; padding: 5px; margin: 5px 0;"> $\mathbf{W}'_{2,1} = \mathbf{W}'_{2,1} \mathbf{W}'_{1,1}$ $\mathbf{b}'_{2,3} = \mathbf{W}'_{2,1} \mathbf{b}'_{1,3} + \mathbf{b}'_{2,3}$ $\mathbf{W}'_{1,3} = \mathbf{W}'_{2,1} \mathbf{W}'_{1,3}$ $\mathbf{W}'_{2,2} = \mathbf{W}'_{2,2} \mathbf{W}'_{1,1}$ $\mathbf{b}'_{2,2} = (\mathbf{W}'_{2,2} \mathbf{b}'_{1,3} + \mathbf{b}'_{2,2}) + \mathbf{W}'_{2,2} \mathbf{W}'_{1,3} \sigma(\mathbf{W}'_{1,2} \mathbf{x}'_0 + \mathbf{b}'_{1,2})$ </div>	$\mathbf{x}'_2 = (\mathbf{W}'_{2,1} \mathbf{x}'_0 + \mathbf{b}'_{2,3}) + UAT_2^R$	$UAT_2^R = \mathbf{W}'_{1,3} \sigma(\mathbf{W}'_{1,2} \mathbf{x}'_0 + \mathbf{b}'_{1,2}) + \mathbf{W}'_{2,3} \sigma(\mathbf{W}'_{2,2} \mathbf{x}'_0 + \mathbf{b}'_{2,2})$
$\mathbf{x}'_3 = (\mathbf{W}'_{3,1} \mathbf{x}'_0 + \mathbf{b}'_{3,3}) + \mathbf{W}'_{1,3} \sigma(\mathbf{W}'_{1,2} \mathbf{x}'_0 + \mathbf{b}'_{1,2}) + \mathbf{W}'_{2,3} \sigma(\mathbf{W}'_{2,2} \mathbf{x}'_0 + \mathbf{b}'_{2,2}) + \mathbf{W}'_{3,3} \sigma(\mathbf{W}'_{3,2} \mathbf{x}'_0 + \mathbf{b}'_{3,2})$ <div style="border: 1px dashed black; padding: 5px; margin: 5px 0;"> $\mathbf{W}'_{3,1} = \mathbf{W}'_{3,1} \mathbf{W}'_{2,1}$ $\mathbf{b}'_{3,3} = \mathbf{W}'_{3,1} \mathbf{b}'_{2,3} + \mathbf{b}'_{3,3}$ $\mathbf{W}'_{1,3} = \mathbf{W}'_{3,1} \mathbf{W}'_{1,3}$ $\mathbf{W}'_{2,3} = \mathbf{W}'_{3,1} \mathbf{W}'_{2,3}$ $\mathbf{W}'_{3,2} = \mathbf{W}'_{3,2} \mathbf{W}'_{2,1}$ $\mathbf{b}'_{3,2} = (\mathbf{W}'_{3,2} \mathbf{b}'_{2,3} + \mathbf{b}'_{3,2}) + \mathbf{W}'_{3,2} \mathbf{W}'_{1,3} \sigma(\mathbf{W}'_{1,2} \mathbf{x}'_0 + \mathbf{b}'_{1,2}) + \mathbf{W}'_{3,2} \mathbf{W}'_{2,3} \sigma(\mathbf{W}'_{2,2} \mathbf{x}'_0 + \mathbf{b}'_{2,2})$ </div>	$\mathbf{x}'_3 = (\mathbf{W}'_{3,1} \mathbf{x}'_0 + \mathbf{b}'_{3,3}) + UAT_3^R$	$UAT_3^R = \mathbf{W}'_{1,3} \sigma(\mathbf{W}'_{1,2} \mathbf{x}'_0 + \mathbf{b}'_{1,2}) + \mathbf{W}'_{2,3} \sigma(\mathbf{W}'_{2,2} \mathbf{x}'_0 + \mathbf{b}'_{2,2}) + \mathbf{W}'_{3,3} \sigma(\mathbf{W}'_{3,2} \mathbf{x}'_0 + \mathbf{b}'_{3,2})$
\vdots \vdots \vdots	\vdots \vdots \vdots	\vdots \vdots \vdots

Figure 12: Some examples of the UAT format of multi-layer Transformer. The changes of parameters are represented within the dashed boxes. The parameters on the right of the equations indicate the original values, while those on the left represent the transformed values. There is no specific order of calculation for the parameters within each dashed box, but there is a top-to-bottom calculation order between different dashed boxes.